Electronic Supplementary Material (ESI) for Journal of Materials Chemistry C.

Supporting Information

Heterointerface Engineering of Tetragonal $CsPbCl_3$ based Ultraviolet Photodetector with Pentacene for Enhancing Photoelectric Performance

Xuning Zhang,[a] Xingyue Liu,[b] Bo Sun,[c] Zhirong Liu,[d] Zhiguo Zhang,[d] Lingxian Kong,[a] Guangliang Li,[c] Mingkui Wang,[d] Zhiyong Liu*,[a] and Guanglan Liao*,[a]

[a] *State Key Laboratory of Digital Manufacturing Equipment and Technology, Huazhong University of Science and Technology, Wuhan, 430074, China.*

[b] *School of Mechanical Engineering and Electronic Information, China University of Geoscience (Wuhan), Wuhan, 430074, China.*

[c] *School of Aerospace Engineering, Huazhong University of Science and Technology, Wuhan, 430074, China.*

[d] *Wuhan National Laboratory for Optoelectronics, Huazhong University of Science and Technology, Wuhan, 430074, China.*

Experimental section

Materials

The ITO substrate with a sheet resistance of 14 Ω^{-1} was purchased from Advanced Election Technology Co., Ltd. Anhydrous ethanol and anhydrous acetone were offered by Sinopharm Chemical Reagent Co., Ltd. Perovskite precursors containing cesium chloride (CsCl, ≥ 99.9%) and lead chloride ($PbCl_2$, ≥ 99.9%) were obtained from Xi'an p-OLED. The pentacene was purchased from Aladdin. All the materials were used directly without further purification.

Device fabrication

First, the ITO/glass substrates were etched followed by the pre-designed pattern. Then, the etched substrates were ultrasonically cleaned by the deionized water, acetone, and anhydrous alcohol in sequence with each process keeping 15 min. After that, they were dried under an N2 flow and illuminated under ultraviolet ozone for 25 min to make sure that there are no residual impurities on the surface. The CsPbCl3 polycrystalline film was synthesized through a sequential vacuum evaporation procedure, where the PbCl2 and CsCl precursors with thicknesses of 200 and 165 nm were evaporated on the ITO substrates at the same speed of 1.5 Å/s under the pressure of 8.0×10-4 Pa. The evaporated speed was traced by a quartz crystal monitor, and the chamber pressure was monitored by a vacuum gauge. To assist crystallization, the as-processed films were annealed at 240 ℃ for 30 min in the ambient air. Finally, the gold electrodes were evaporated above the samples with a thickness of 40 nm at a speed of 0.6 Å/s under the pressure of 6.0×10-4 Pa. For the construction of the photodetector arrays, the top-contact electrode array was constructed under the assistance of a pre-designed metal mask with a pixel scale of 600×600 μm.

Materials Characterizations

The absorption spectra of the CsPbCl3 and pentacene films were tested via a UV-vis spectrophotometer (UV 2600, Shimadzu, Japan). The X-ray diffraction (XRD) spectrum of the CsPbCl3 film was measured by an x'pert3 powered X-ray diffractometer (PANalytical, Netherland) with a scanning step of 0.013°. The surface morphologies and roughnesses of the CsPbCl3 and pentacene films were characterized by scanning electron microscopy (Nova NanoSEM 450, FEI, Netherlands) and atomic force microscopy (AFM, Innova SPM 9700, Shimadzu, Japan). The measurements of X-ray photoelectron spectroscopy (XPS) and ultraviolet photoelectron spectroscopy (UPS) were carried out on a photoelectron spectrometer

(AXIS-ULTRA DLD-600W, Kratos, Shimadzu, Japan). The steady-state and time-resolved photoluminescence (PL) were surveyed by the QuantaMaster 800 (HORIBA, Canada) under the excitation lights of a 365 nm xenon lamp and 340 nm laser, respectively.

Device Characterizations

For the spectral characteristics of the photodetectors, the incident photon to current conversion efficiency (IPCE) was obtained under the illumination of monochromatic lights from a xenon lamp coupled with a monochromator (TLS1509, Zolix). The photo response to the incident light intensities was explored based on a four-probe station (ECPS400) system, which contains a function/arbitrary waveform generator (Keysight 33210A) and a source meter (Keithley 2636B) to modulate the illuminated model of the LED and record the response of the devices. The intensity of the LED can be tailored by changing the driving voltage and the distance between the LED and the photodetectors. Under a fixed driving voltage of 18 mV, the light intensities vary from 12.5 mW/cm2 to 246 nW/cm2 among the distances of 6-13 cm. The dark and light currents are recorded without external bias in the ambient air. The response times were derived from the temporal response by an oscilloscope (Tektronix, TDS2012B). Rejection ratios of the ultraviolet to visible lights were obtained from the response under light illuminations of 375, 450, 520, and 637 nm.

Computational details

Calculations of the optical and electronic properties were performed within the density-functional theory framework using the CASTEP package. The tetragonal CsPbCl3 crystal with lattice constants of $a = b = 5.590$ Å , $c = 5.630$ Å , and $\alpha=\beta=\gamma=90^{\circ}$ was used in the theoretical calculations. The projected augmented wave (PAW) approximation and Perdew Burke Ernzerhof (PBE)-generalized gradient approximation (GGA) were chosen to deal with the ion-electron interactions and exchange-correlation functional, respectively. K-grids of 2×2×2 and cutoff energy of 400 eV were used in structure relaxation. The structural parameters of the CsPbCl3 were determined using several optimum minimization techniques which have already been embedded within the user code. It is also the fastest way to reach convergence. The calculations were carried out under some conditions: the tolerance of geometrical optimization was represented by the change of total energy with 1×10-5 eV per atom, maximum ionic Hellmann-Feynman force with 0.03 eV/Å, maximum stress with 0.05 GPa, and maximum ionic displacement with 1×10-3 Å.

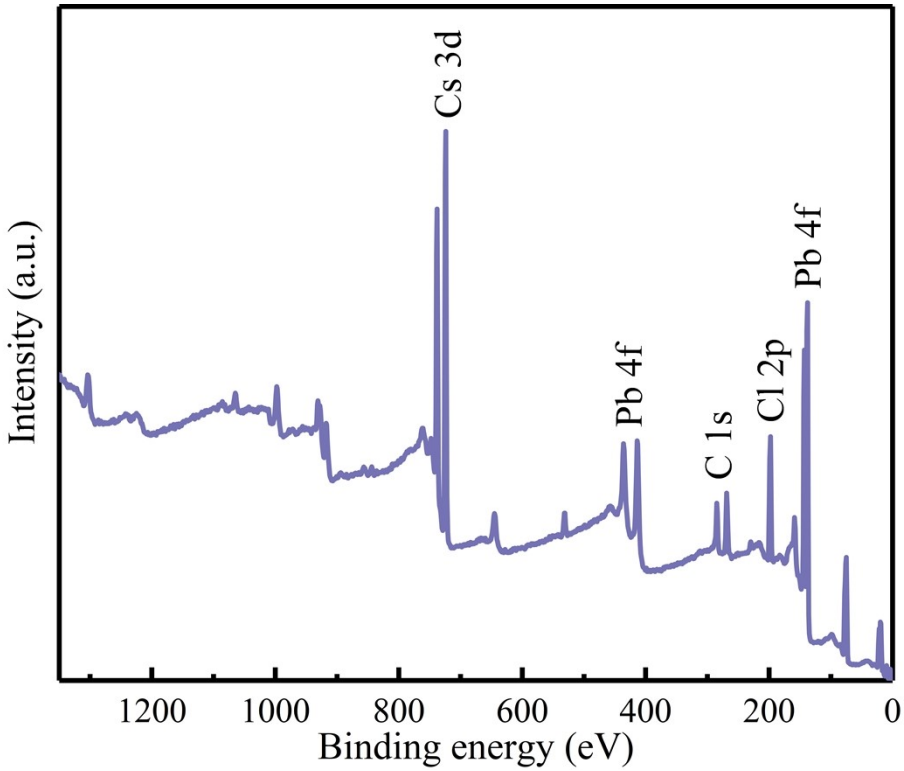

Figure S1: X-ray photoelectron spectroscopy (XPS) spectrum of the evaporated $CsPbCl_3$ polycrystalline film.

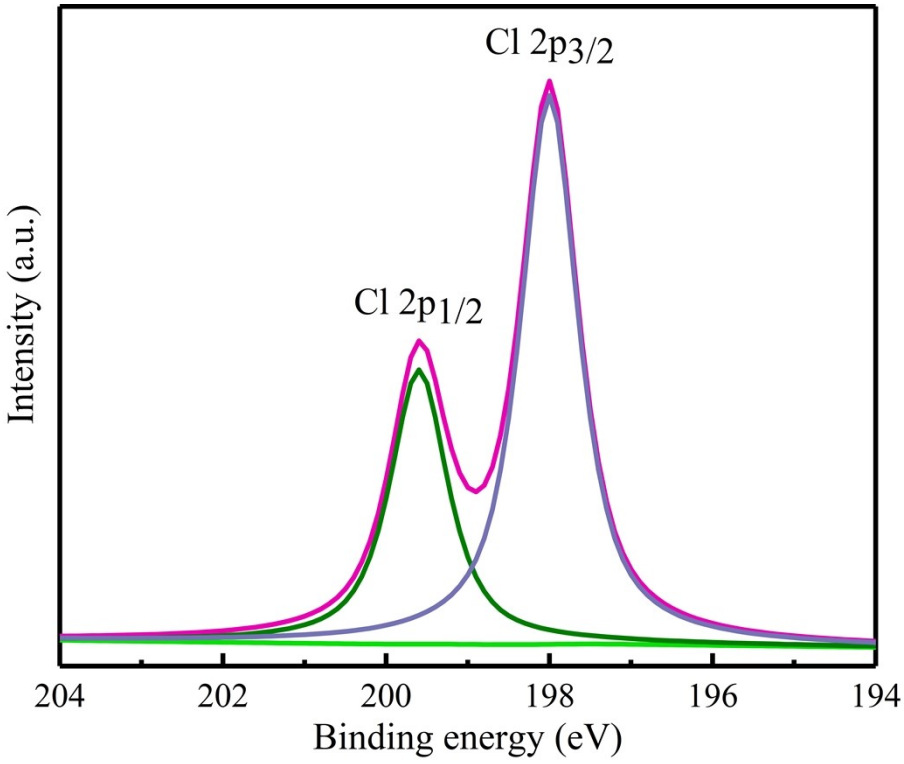

Figure S2: High-resolution XPS spectra of Cl 2p.

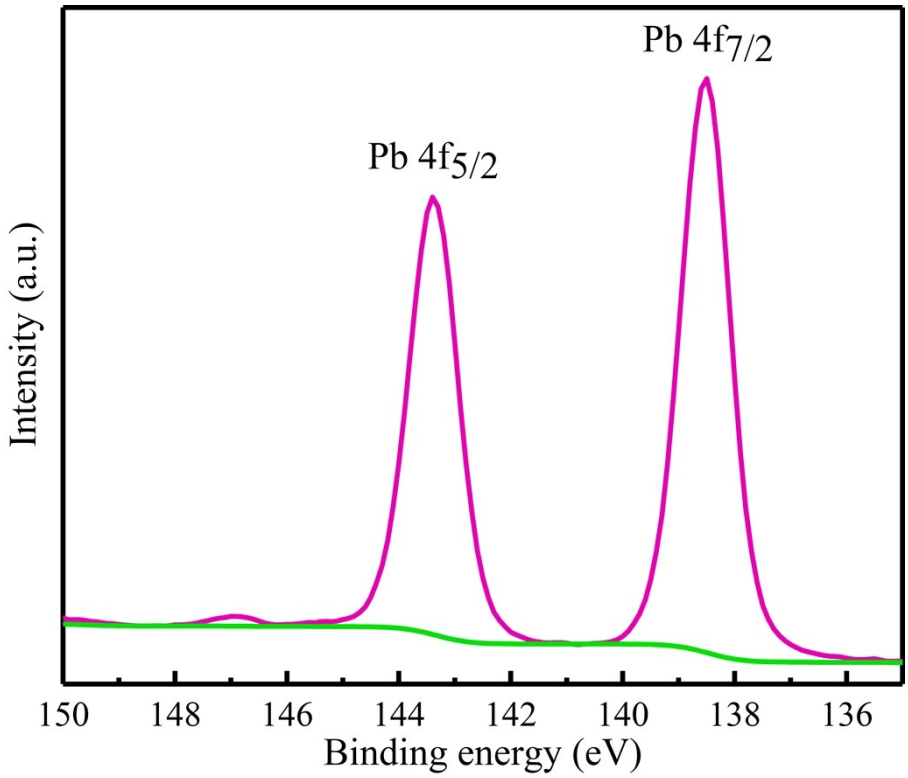

Figure S3: High-resolution XPS spectra of Pb 4f.

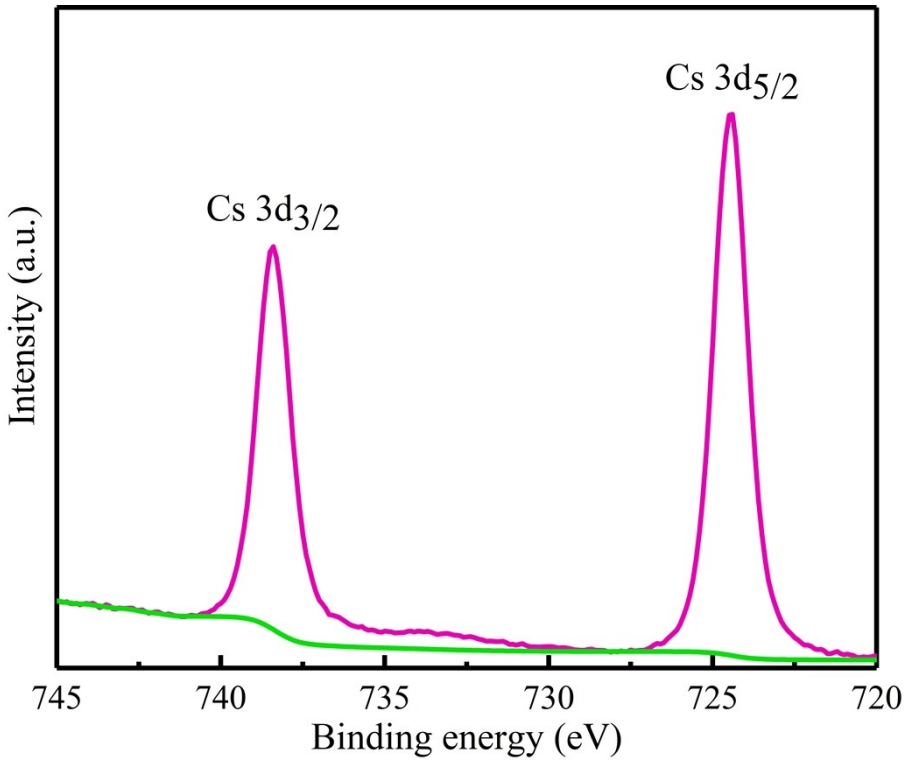

Figure S4: High-resolution XPS spectra of Cs 3d.

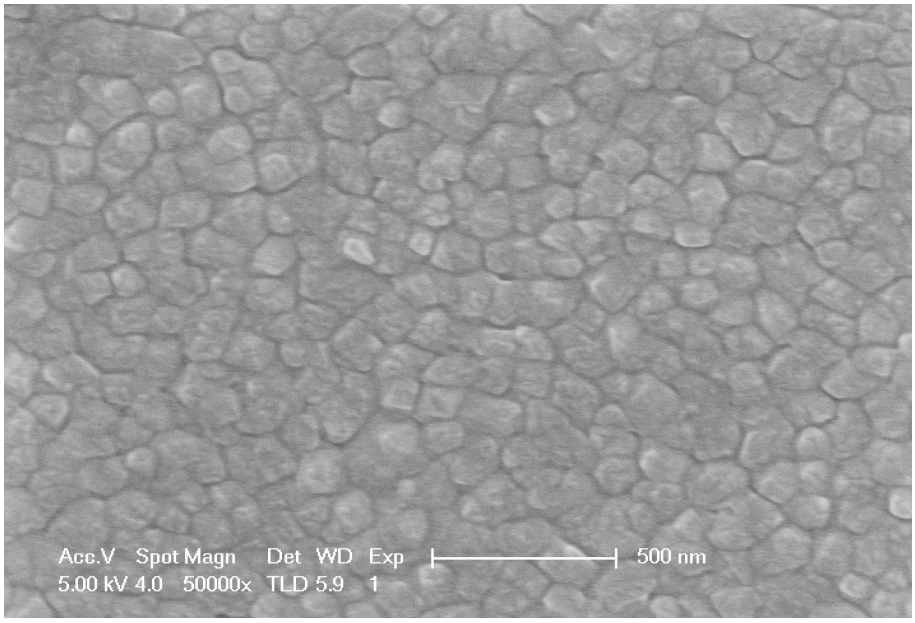

Figure S5: Scanning electron microscope (SEM) image of the evaporated pentacene film.

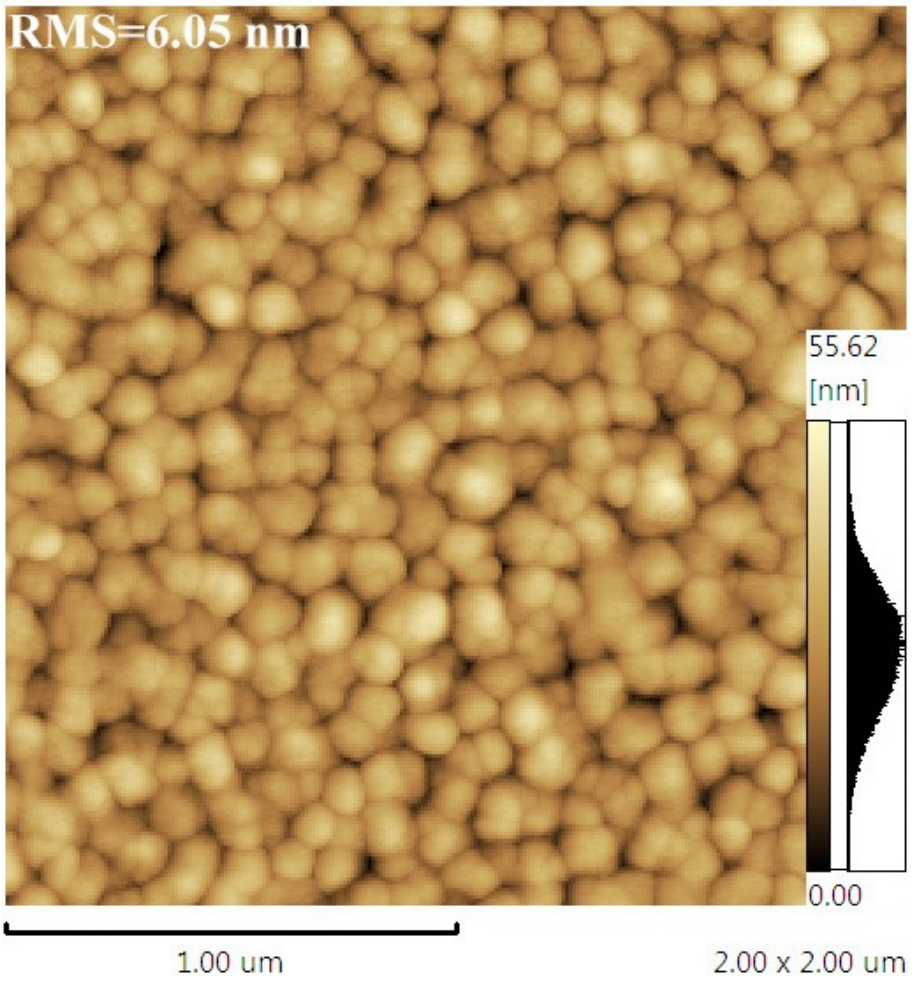

Figure S6: Atomic force microscope (AFM) image of the evaporated pentacene film.

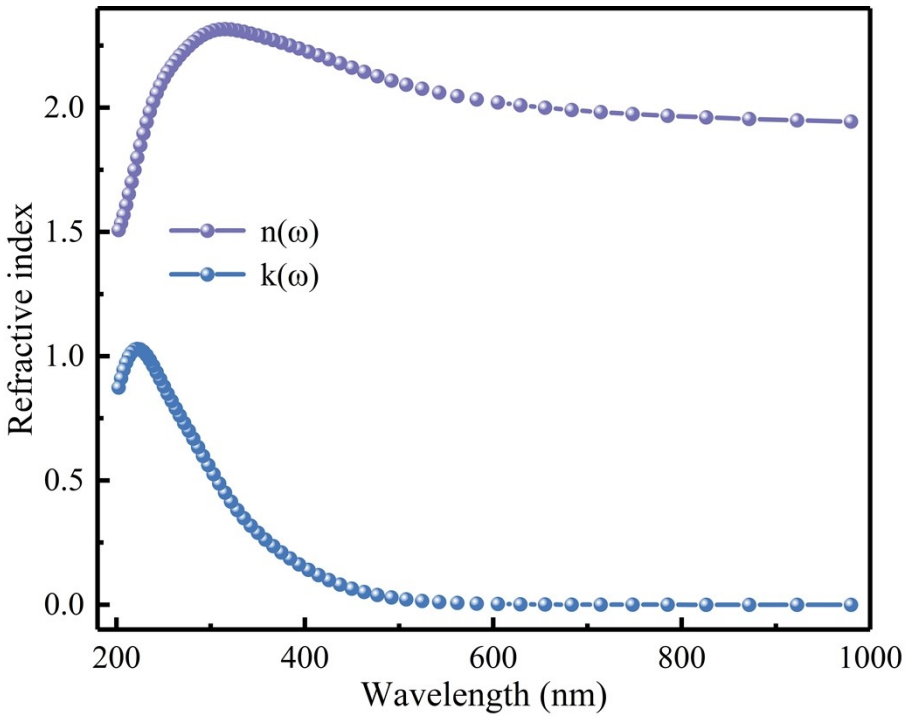

Figure S7: The reflectivity spectrum of $CsPbCl_3$ by DFT calculations.

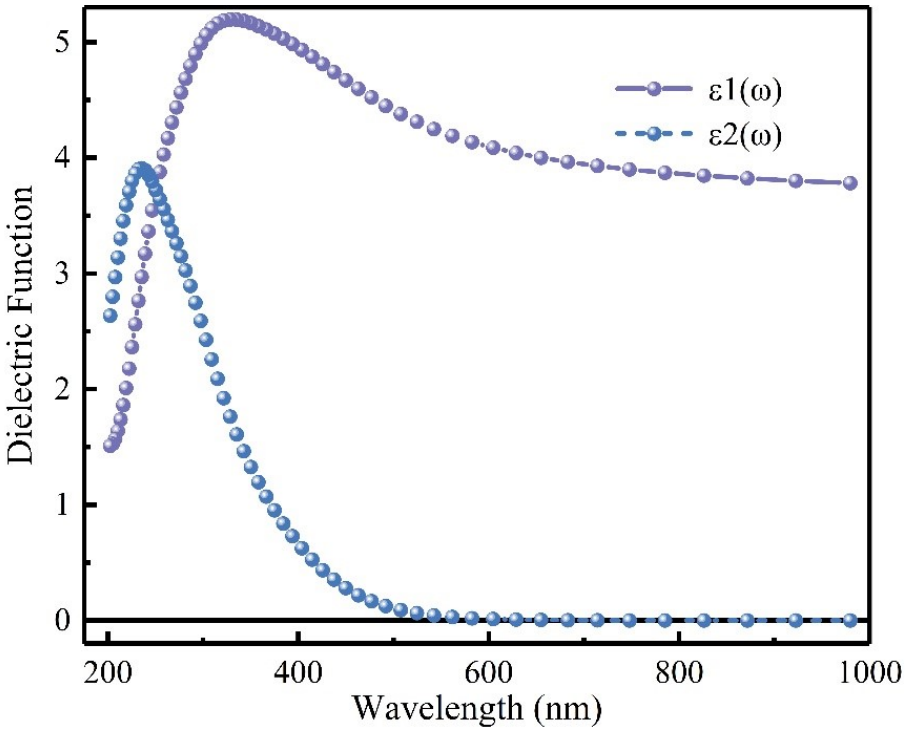

Figure S8: The Real, $\varepsilon_1(w)$ and Imaginary $\varepsilon_2(w)$ parts of the dielectric function of $CsPbCl_3$ by DFT calculations.

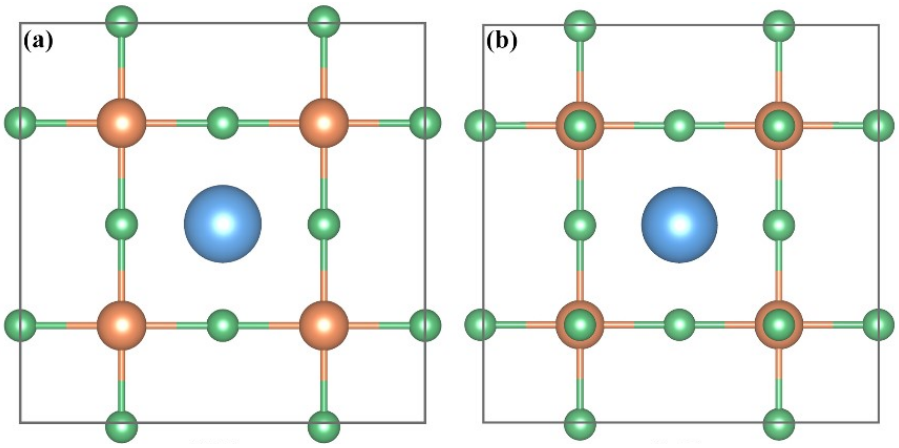

Figure S9: Slab models of $CsPbCl_3$ (a) (100)-$PbCl_2$ terminal, (b) (100)-CsCl terminal, showing a rectangle with length and width of 11.324456 and 11.324681 Å.

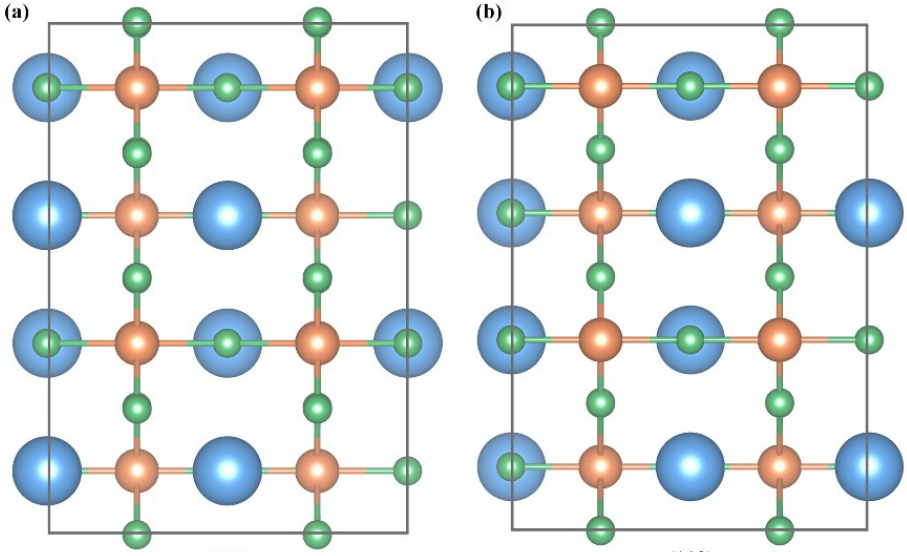

Figure S10: Slab models of $CsPbCl_3$ (a) (110)-Cl terminal, (b) (110)-$PbCl_2$ terminal, showing a rectangle with length and width of 11.324681 and 16.015199 Å.

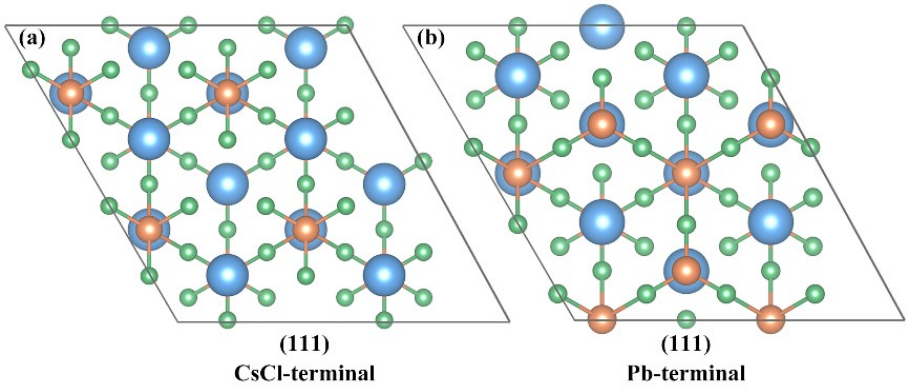

Figure S11: Slab models of $CsPbCl_3$ (a) (111)-CsCl terminal, (b) (111)-Pb terminal, showing a parallelogram with side lengths of 16.015199, 16.015358 Å and an angle of 119.99967°.

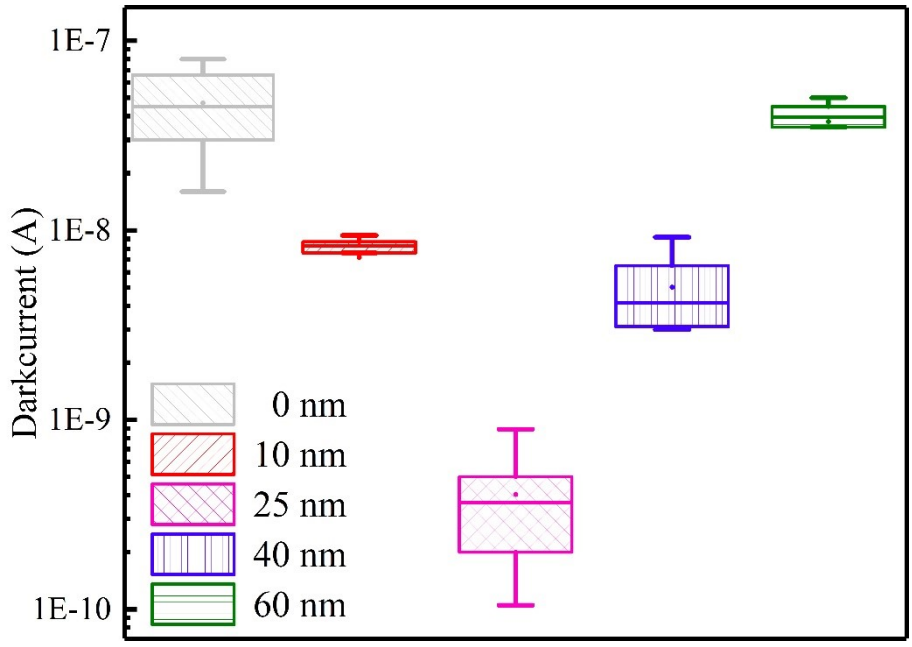

Figure S12: Dark currents of the photodetectors based on the $CsPbCl_3$-Pentacene hybrid structure with different thicknesses of the pentacene film.

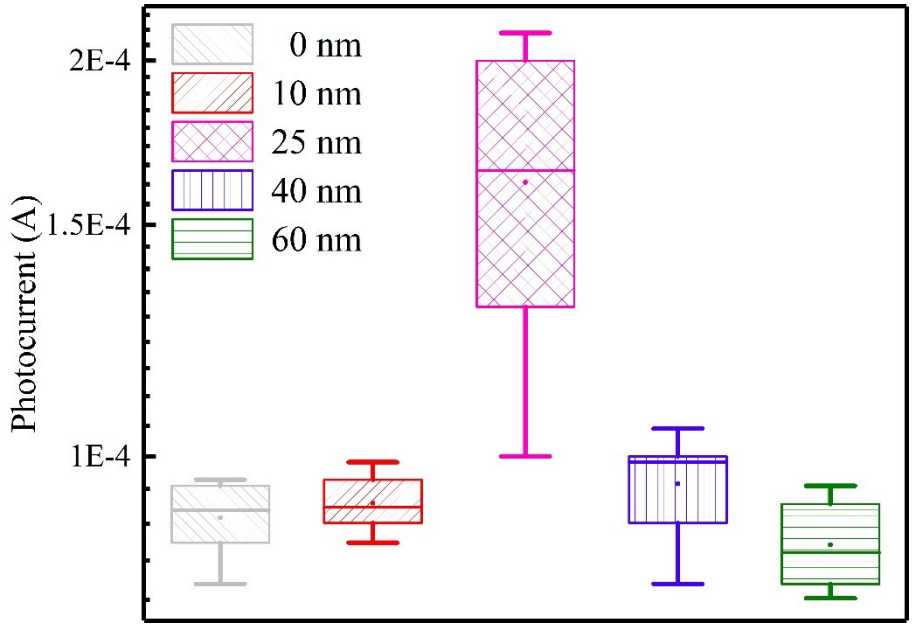

Figure S13: Photo currents of the photodetectors based on the $CsPbCl_3$-Pentacene hybrid structure with different thicknesses of the pentacene film.

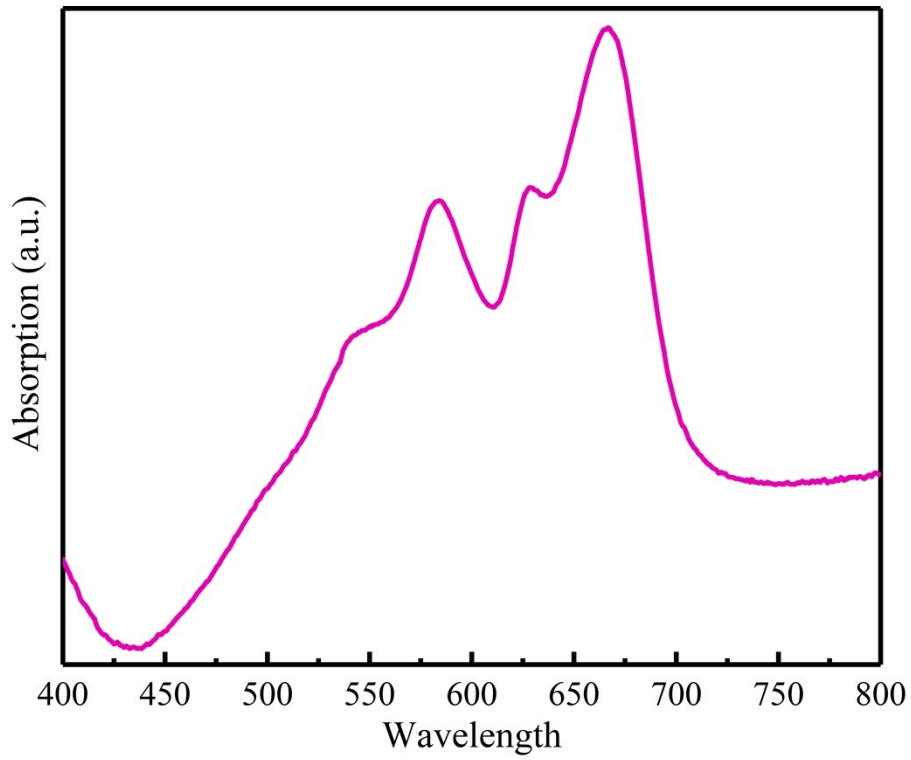

Figure S14: Absorption spectrum of the pentacene film.

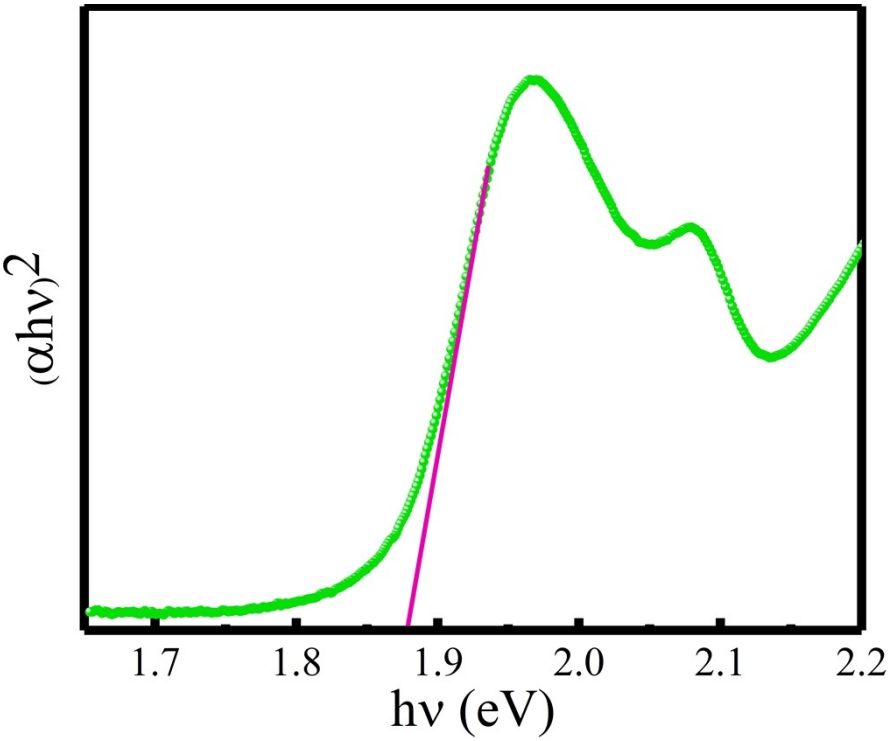

Figure S15: Tauc-plot for the pentacene film based on the absorption spectrum.

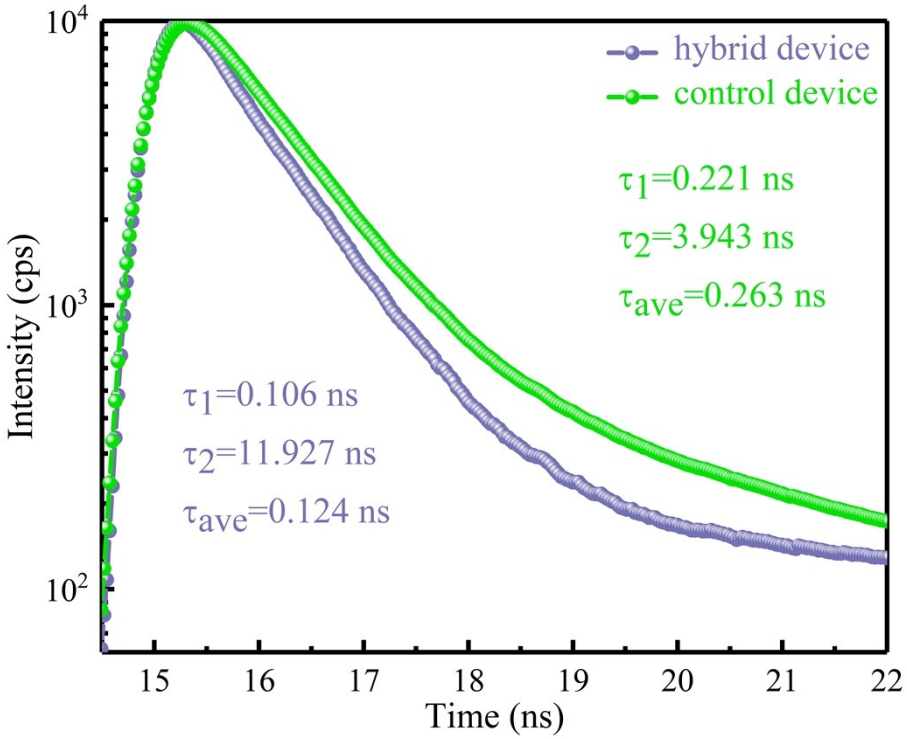

Figure S16: Time-resolved photoluminescence (TRPL) spectra for the $CsPbCl_3$ (green spheres) and $CsPbCl_3$-Pentacene hybrid films (purple spheres).

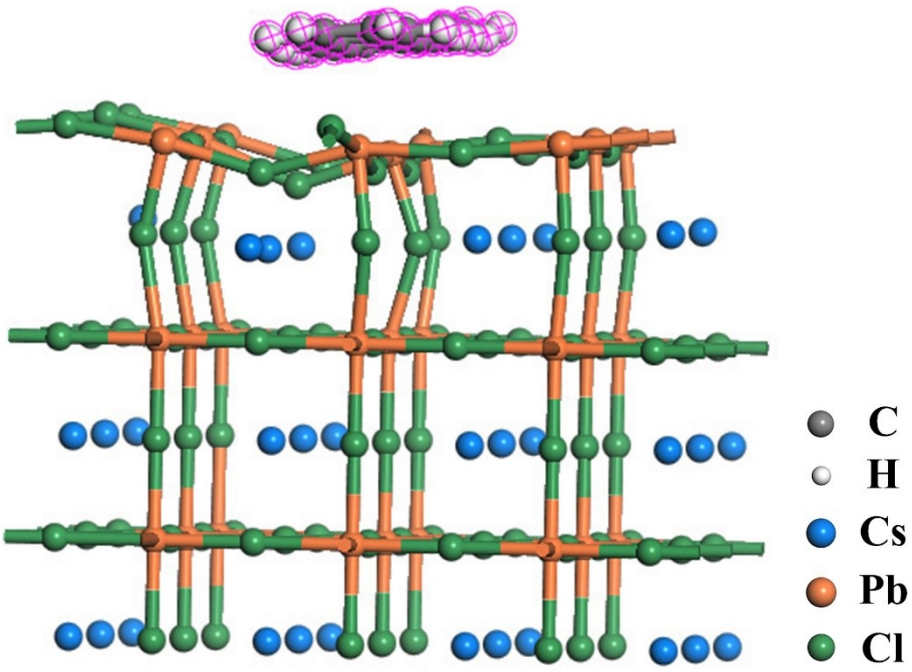

Figure S17: Relaxed structure diagram based on the small molecule absorption model.

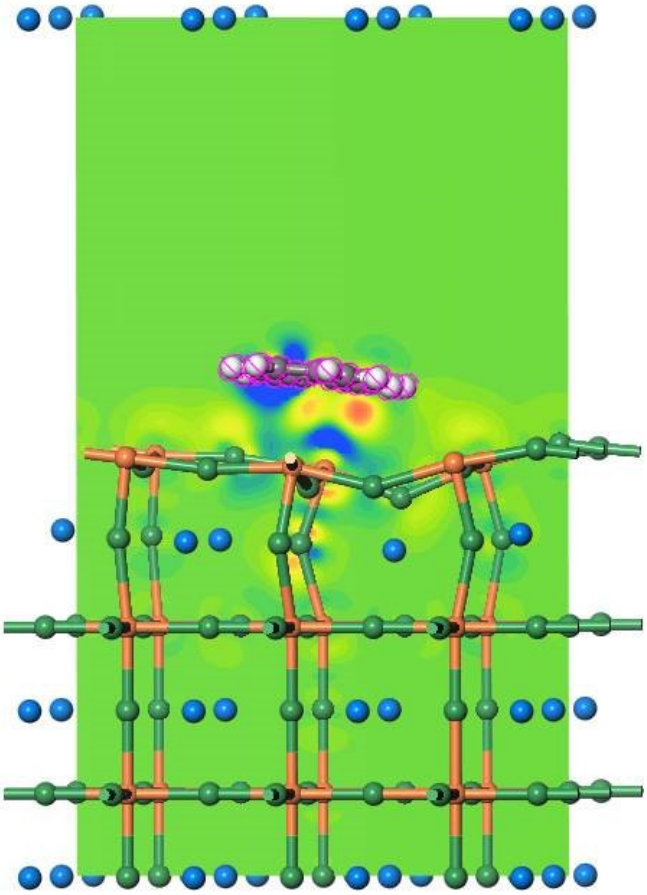

Figure S18: Sliced map of the charge density difference along the direction of (010).

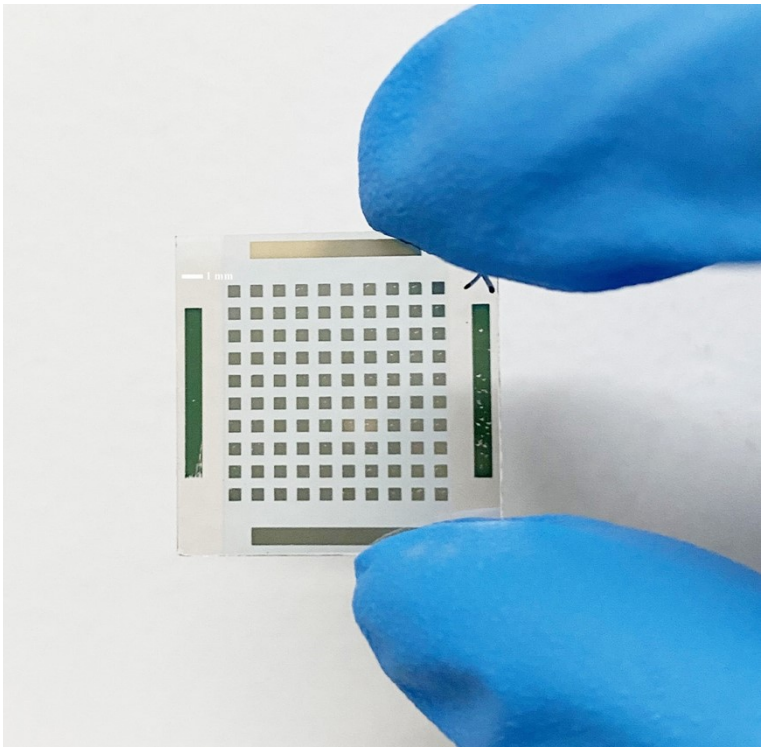

Figure S19: Optical image of the arrayed photodetectors.

Table S1: X-ray photoelectron spectroscopy (XPS) results of the evaporated $CsPbCl_3$ film.

Name	Start BE	Peak BE	End BE	FWHM	Atomic %
Pb 4f	153.84	138.52	134.04	1.04	11.57
Cl 2p	210.84	198.02	191.04	0.98	35.16
Cs 3d	745.84	724.46	717.04	1.23	12.39
C 1s	298.84	284.80	280.04	1.27	40.88

Table S2 Peak position information on the XRD spectrum of the $CsPbCl_3$ film.

Number	Peak position	Interplaner spacing	Miller indices
	2 Theta (°)	d (Å)	(h k l)
1	15.8126	5.6000	(1 0 0)
2	22.4792	3.9520	**(1 0 1)**
3	32.0149	2.7933	**(2 0 0)**
4	35.9038	2.4993	(2 0 1)
5	39.4278	2.2835	(2 1 1)
6	45.8872	1.9760	(2 2 0)

Table S3: Convergence tests on the k-points under a fixed cutoff energy of 550 eV.

	K-points	Initial Volume ($Å^3$)	Final Volume ($Å^3$)	Deviation (%)
1	1×1×1	175.926803	166.722658	0.0540
2	2×2×2	175.926803	181.471924	**0.0315**
3	3×3×3	175.926803	186.836526	0.0620
4	4×4×4	175.926803	188.142020	0.0694

Table S4: Convergence tests on the cutoff energy under fixed k-points of 2×2×2.

	Cutoff energy (eV)	Initial Volume ($Å^3$)	Final Volume ($Å^3$)	Deviation (%)
1	300	175.926803	181.944156	0.0340
2	350	175.926803	181.599201	0.0322
3	400	175.926803	181.468291	**0.0314**
4	450	175.926803	181.525401	0.0318
5	500	175.926803	181.839561	0.0319

Table S5: Atomic populations (Mulliken).

species	Ion	s	p	d	Total	Charge
Cl	1	1.96	5.52	0.00	7.48	-0.48
Cl	2	1.96	5.52	0.00	7.48	-0.48
Cl	3	1.96	5.52	0.00	7.48	-0.48
Cs	1	2.03	5.93	0.16	8.11	0.89
Pb	1	4.15	7.30	10.00	21.45	0.55

Table S6: Bond populations.

Bond	Population	Length
Cl 1 - Pb 1	0.56	2.82497
Cl 3 - Pb 1	0.56	2.83090
Cl 2 - Pb 1	0.56	2.83090
Cl 3 - Cs 1	-0.13	3.99280
Cl 2 - Cs 1	-0.13	3.99280
Cl 1 - Cl 3	-0.05	3.99858
Cl 1 - Cl 2	-0.05	3.99858

Table S7: Surface energies of $CsPbCl_3$ along different planes.

Miller indices	Slab area	Terminal type	Molecules	Relaxed energy	Bulk Energy	Surface energy
	S ($\mathring{A}^2$)		n	E_{slab} (eV)	E_{bulk} (eV)	$E_{surface}$ (eV)
(1 0 0)	S_{100}	PbCl2	12	-89742. 5720	-7479.1580	**0.0285**
		CsCl	12	-89742. 4903	-7479.1580	**0.0288**
(1 1 0)	S_{110}	Cl	12	-89732.5192	-7479.1580	0.0338
		PbCl2	12	-89732.2507	-7479.1580	0.0344
(1 1 1)	S_{111}	CsCl	12	-89734.1704	-7479.1580	0.1001
		Pb	12	-89732.6119	-7479.1580	0.1100